Electrorheological Semiactive Shock Isolation Platform for Naval Applications

authored by **W. Kemmetmüller, K. Holzmann, A. Kugi, and M. Stork**

and published in *IEEE/ASME Transactions on Mechatronics*.

Cite this article as:

W. Kemmetmüller, K. Holzmann, A. Kugi, and M. Stork, "Electrorheological Semiactive Shock Isolation Platform for Naval Applications", *IEEE/ASME Transactions on Mechatronics*, vol. 18, no. 5, pp. 1437–1447, 2013. DOI: 10.1109/TMECH.2012.2203456

BibTex entry:

```
% This file was created with JabRef 2.9.2.
% Encoding: Cp1252

@ARTICLE{acinpaper,
  author = {Kemmetmüller, W. and Holzmann, K. and Kugi, A. and Stork, M.},
  title = {Electrorheological {S}emiactive {S}hock {I}solation {P}latform for
        {N}aval {A}pplications},
  journal = {IEEE/ASME Transactions on Mechatronics},
  year = {2013},
  volume = {18},
  pages = {1437-1447},
  number = {5},
  doi = {10.1109/TMECH.2012.2203456}
}
```

Link to original paper:

http://dx.doi.org/10.1109/TMECH.2012.2203456

Contact:

Automation and Control Institute (ACIN)
Vienna University of Technology
Gusshausstrasse 27-29/E376
1040 Vienna, Austria

Internet: www.acin.tuwien.ac.at
E-mail: office@acin.tuwien.ac.at
Phone: +43 1 58801 37601
Fax: +43 1 58801 37699

Electrorheological Semi-active Shock Isolation Platform for Naval Applications

Wolfgang Kemmetmüller, *Member, IEEE,* Klaus Holzmann, Andreas Kugi, *Member, IEEE,* and Michael Stork

***Abstract*—This paper presents a semi-active shock absorber system which utilizes the special properties of electrorheological (ER) valves and which is intended to protect sensitive equipment on ships or submarines. It consists of a platform and a base plate, which are connected via an ER damper and an air spring. The resulting acceleration of the platform upon an external shock of the base plate should be significantly reduced while assuring fast and accurate repositioning of the platform after the shock. A control strategy is discussed, which fulfills these requirements using only one acceleration sensor. Simulation studies and measurement results on a prototype prove the feasibility of the proposed system.**

***Index Terms*—Electrorheological fluid, shock absorber, semi-active shock isolation, modeling.**

I. Introduction

THE broad topic of vibration and shock isolation is of great interest in many technical applications, with the objective of reducing the effect of external excitations in some manner. The present work in particular considers short individual events of (in some range) unknown strength that can occur at unknown times, so-called shocks [1]. The goal of shock isolation platforms is to avoid negative effects on plants, devices, goods or persons, which are exposed to the shock. In case of plants or devices, it might be possible to modify them mechanically, thus making them insensitive to high accelerations. This approach is not applicable to goods or persons, thus an alternative approach is necessary in order to avoid damage or injuries. Therefore, suitable shock isolators are frequently used in order to protect goods and persons. These systems also allow for the use of conventional standard devices, which often results in a lower price of the overall system.

This work deals with a semi-active shock isolation platform intended to be used on ships or submarines to increase their resistance against shocks from different sources including weaponry impact [1]. Shocks of this type are characterized by very high accelerations up to $3000\ \mathrm{m/s^2}$ and a short duration of less than 100 ms. The objective of the shock isolation platform is to significantly reduce the acceleration induced by a high vertical shock on the base plate (i.e. the ship) and to assure a fast and accurate repositioning of the platform after a shock. Furthermore, the system has to be well damped in order to prevent undesired motion of the platform in normal operation e.g. due to the motion of the sea.

Shock isolators for marine applications are frequently based on wire rope isolators [2]. In case of a shock, the deformation of the wire ropes significantly decreases the resulting accelerations on the platform. However, such systems suffer from the disadvantage that the difference in the position between the platform and the base plate before and after the shock is often larger than allowed, i.e. the required repositioning cannot be achieved. Alternatively, passive damping systems consisting of a spring in parallel with a damper are frequently used, both with a fixed characteristics. With these passive elements with fixed characteristics it is impossible to fulfill both the requirements of the shock isolation and the fast repositioning during normal operation. A special configuration of passive elements are elastomer vibration isolators, which combine the functions of a spring and a damper in one element [3].

Although these existing solutions provide some basic isolation of the platform with respect to shocks, the conflicting demands on shock isolation and high damping in normal operation cannot be completely satisfied. Therefore, adjustable dampers are used in this paper in order to improve the quality of shock isolation of these simple concepts. The proposed concept is based on the specific properties of so-called electrorheological (ER) fluids (ERF). Such fluids are in general suspensions of polarizable solid particles in a fluid phase [4]. Without an external electrical field such a fluid behaves rheologically like a normal Newtonian fluid of a given dynamic viscosity. Upon application of a sufficiently large electrical field, the particles form chains or agglomerate in some manner [4]. These chains are responsible for the reversible and fast change in the rheological properties, i.e. the apparent viscosity of the ERF. By using semi-active dampers which are based on the ER effect, a new type of shock isolation platform has been designed which significantly improves the behavior of the system during shock and in normal operation. Furthermore, it is shown in this paper that only the exploitation of the special properties of electrorheological fluids with a mechatronic design of the overall system allows to reach the desired goals of the shock isolation platform.

The paper is organized as follows: Section II describes the proposed concept for the semi-active shock isolation platform. This is followed by the mathematical modeling of the platform

This work was supported by the Bundeswehr Research Institute for Materials, Fuels and Lubricants (WIWeB), Erding, Germany.

W. Kemmetmüller is with Automation and Control Institute (ACIN), Vienna University of Technology, 1040 Vienna, Austria (e-mail: kemmetmueller@acin.tuwien.ac.at).

K. Holzmann was with the Automation and Control Institute (ACIN), Vienna University of Technology, 1040 Vienna, Austria. He is now with Fludicon GmbH, 64293 Darmstadt, Germany (e-mail: klaus.holzmann@fludicon.com).

A. Kugi is with Automation and Control Institute (ACIN), Vienna University of Technology, 1040 Vienna, Austria (e-mail: kugi@acin.tuwien.ac.at).

M. Stork is with Fludicon GmbH, 64293 Darmstadt, Germany (e-mail: michael.stork@fludicon.com).

Manuscript received June 1, 2012.

Post-print version of the article: W. Kemmetmüller, K. Holzmann, A. Kugi, and M. Stork, "Electrorheological Semiactive Shock Isolation Platform for Naval Applications", *IEEE/ASME Transactions on Mechatronics*, vol. 18, no. 5, pp. 1437–1447, 2013. doi: 10.1109/TMECH.2012.2203456
The content of this post-print version is identical to the published paper but without the publisher's final layout or copy editing.

and its components in Section III and by a discussion of the control strategy in Section IV. The usefulness and the feasibility of the proposed semi-active shock isolation platform with the corresponding control strategy are shown by means of simulation results in Section V and by means of measurement results in Section VI.

II. Concept

In order to prove the basic idea of the electrorheological semi-active shock isolation platform, a system with one degree-of-freedom has been designed which can only cope with vertical excitations. The concept of this one-dimensional platform is based on the principle of semi-active suspensions comprising a spring in parallel to an adjustable damper [5], see Fig. 1. The system consists of a base plate (position z_B, velocity v_B and acceleration a_B) directly connected to the ship and a shock isolation platform (position z_P, velocity v_P and acceleration a_P) whose acceleration should be kept as small as possible.

The spring has to compensate the static load of the platform and all components connected to it including the goods placed on it. If a classical steel spring would be used, the fixed pre-load of the spring would result in different positions z_P of the platform if the static load of the platform is changed. Therefore, air springs which allow to adjust the pre-load by means of the pressure p_A are used in this project. The damping of the system is provided by damping cylinders with chamber pressures p_1 and p_2, whereby the damping can be adjusted by a suitable control of the voltage U applied to the ER-valve. The platform is assumed to be ideally stiff and hence it can be modeled as a rigid body. Furthermore it is assumed that the excitation a_B of the ship acts only vertically.

The considered field of application of the shock isolation platform on ships and submarines is characterized by the following two scenarios: (i) In normal operation, the only excitation of the platform is due to the motion of the ship or due to the change of the static load. In this situation, no reduction of the acceleration of the platform is necessary but the relative position between the base plate and the platform $z_P - z_B$, i.e. the relative position of the platform to the ship, has to be kept as constant as possible. Therefore, very high damping of the motion of the platform is necessary. (ii) In the case of a shock on the base plate, the acceleration of the platform has to be kept as low as possible which in turn means that the forces on the platform should be minimized. This yields a minimization of the actual damping force during the shock. However, directly after the shock, which in general is a very short event, the damping has to be increased again in order to obtain fast repositioning of the platform.

Based on these two scenarios, the ER damper has to bridge the gap between very different amounts of damping. Since the most important feature of the shock isolation platform is to protect the equipment, the ER damper has been designed based on the requirements of the shock scenario. Very large volume flows occur during a shock which leads to a rather large geometry of the ER valve. This, however, makes it difficult to accurately control the relatively small volume flows

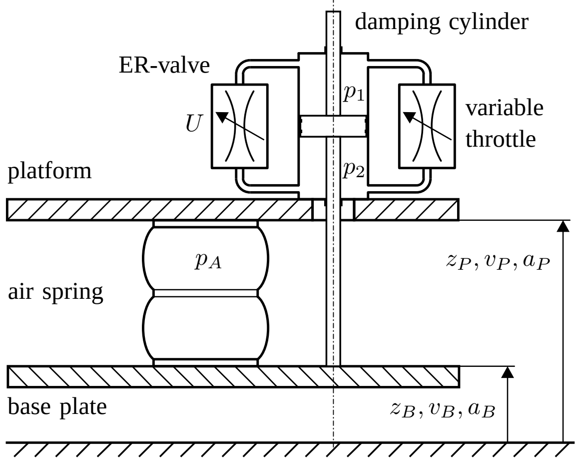

Fig. 1. Concept of the semi-active shock isolation platform.

and therefore the damping during low excitations in normal operation, e.g. caused by water waves acting on the ship. (ii) Thus, the damping of the platform during normal operations is defined by a small (passive) bypass throttle which is connected in parallel to the ER-valve. In normal operation the ER valve is closed and only the bypass throttle is active which yields a fast repositioning of the platform after the shock and sufficient damping in normal operation.

Using only one damper and spring element as depicted in Fig. 1 would lead to asymmetric forces on the platform. Furthermore, the rather large mass of the platform would result in quite large components (ER-valve, damping cylinder and air spring). For this reason, each of the four corners of the platform is equipped with a spring and a semi-active ER-damper, where the control of the four ER dampers is synchronized.

As already outlined, ER-valves are used in order to adjust the damping of the semi-active damper. Naturally, other constructions using e.g. conventional proportional valves would be imaginable. The use of ER-technology, however, provides some major advantages for this type of application: (i) The dynamics of the ER-valve is determined by the fast dynamics of the ERF (in the range of a few milliseconds) which can hardly be reached with classical electrohydraulic valves. (ii) The ER-valve can be closed by applying a voltage without moving any mechanical components. If in the case of a shock the control fails and the ER-valve is kept closed, the ER-valve will still open if the pressure difference along the valve exceeds a certain limit. This property of an ER valve results from the fact that an ER fluid can only generate a limited yield strength. Thus, also the forces on the platform are limited and even in this case the accelerations on the platform are significantly reduced. If, however, a conventional proportional valve would have been used, keeping the valve closed in the case of a shock would result in very high accelerations of the platform and, in worst case, to a damage of the shock isolation platform.

Post-print version of the article: W. Kemmetmüller, K. Holzmann, A. Kugi, and M. Stork, “Electrorheological Semiactive Shock Isolation Platform for Naval Applications”, *IEEE/ASME Transactions on Mechatronics*, vol. 18, no. 5, pp. 1437–1447, 2013. doi: 10.1109/TMECH.2012.2203456
The content of this post-print version is identical to the published paper but without the publisher’s final layout or copy editing.

III. Mathematical Modeling

The essential part of the shock isolation platform is the electrorheological semi-active damper, see, e.g., [6]. The semi-active damper consists of the damping cylinder together with the ER-valve, the bypass throttle and the piping, see Fig. 2. Due to the design of the ER-valve, a small constant volume exists at both ends of the ER-valve with the corresponding pressures p_{V1} and p_{V2}. The mass flows between the damping cylinder and these volumes are $\dot{m}_1$ and $\dot{m}_2$ while the mass flows through the ER-valve and the bypass throttle are denoted by $\dot{m}_{ER}$ and $\dot{m}_T$, respectively.

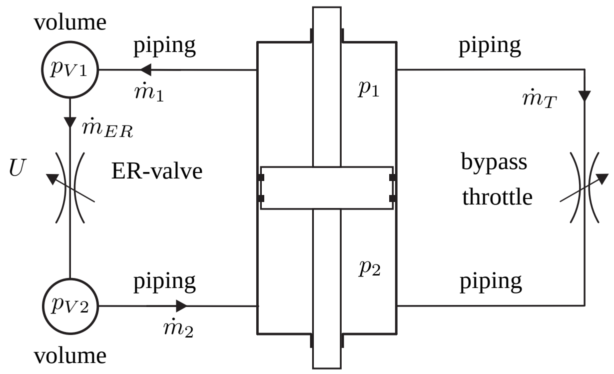

Fig. 2. Hydraulic diagram of the semi-active damper.

The ER-damper uses an electrorheological fluid, which, as already mentioned, changes its apparent viscosity upon application of an electric field. In the absence of an external electric field the ERF behaves like a normal fluid, such that in all components but the ER-valve the ERF can be described by an isentropic compressible fluid model which is derived in Section III-A. In these parts, the dominating effects are due to the (changing) compressibility of the ERF and the effects of the very low viscosity of the ERF can be neglected. The special field dependent properties of the electrorheological fluid are addressed afterwards in Section III-B which is concerned with the mathematical modeling of the ER-valve. The model is completed by a mathematical description of the damping cylinder, the piping, the air spring and the motion of the platform given in Sections III-C to III-F.

A. Isentropic Fluid

The bulk modulus β of an isentropic fluid is defined by

$$\beta = \beta_0 = \rho \frac{\partial p}{\partial \rho}, \tag{1}$$

with the pressure p and the mass density ρ, cf. [7], [8], [9]. The assumption of a constant bulk modulus $\beta = \beta_0$ is very well satisfied, if (i) the pressure p is below 1000 bar and (ii) the pressure p is above a certain saturation pressure p_{sat}, which is in the range of $1\,\mathrm{bar}$. Both assumptions are typically satisfied in conventional hydraulic systems. In the present application of the fluid, the shock isolation platform, the second assumption will not be satisfied in the case of a shock event. In this case, the high accelerations result in very large volume flows which in turn can cause that the pressure in some parts of the system drops significantly below the saturation pressure p_{sat}. Therefore, a mathematical model for an isentropic fluid will be derived in this section which gives a correct description of the fluid behavior even in this case.

If the pressure drops below the saturation pressure p_{sat} then a significant reduction of the bulk modulus β and of the mass density ρ occurs. There are basically two reasons which are responsible for this effect: (i) In technical applications it is inevitable that the oil gets in contact with the air. During transport, storage or normal use, air can be partially dissolved within the hydraulic oil. If the pressure drops below a certain level, the previously dissolved air is partially set free in the form of gas bubbles, cf. [10]. (ii) Even if the fluid would be free of dissolved air, a further decrease of the pressure leads to a vaporization of the fluid itself (cavitation, see, e.g., [11]). These gas bubbles and the vapor of the fluid are responsible for the dramatic decrease of the bulk modulus and the mass density in this case. As already mentioned, cavitation is avoided in most applications of conventional hydraulics. It is, however, part of operation of the shock isolation platform presented in this contribution. In order to correctly describe the behavior of the platform, the mathematical model of the fluid must incorporate the effects described above [11].

The saturation pressure p_{sat} is the smallest pressure, at which the whole air is dissolved within the fluid in the stationary case [12], whereby it is assumed that the dissolved gas incorporates no volume. Below this saturation pressure, in the stationary state the gas is partially or completely free. The upper limit, i.e. the pressure at which the evaporation of the fluid starts, is referred to as the upper saturation vapor pressure p_{vapU}. In a chemical pure substance, all dissolved air would be free below p_{sat} and all fluid would be evaporated below p_{vapU}. Of course, the ERF used in this project is not a chemical pure substance. Thus, these processes occur over a finite pressure range. It should be pointed out that only equilibrium states are considered. It is also assumed that the air below the upper saturation vapor pressure p_{vapU} is completely free and thus the release of dissolved air and the evaporation of the hydraulic fluid occur within different pressure regimes. With the assumption $p_{vapL} < p_{vapU} < p_{sat}$ one can distinguish the following four cases:

1) $p_{sat} < p$: No vapor is present and all of the air is dissolved within the fluid.
2) $p_{vapU} < p \leq p_{sat}$: No vapor is present and the air is partially dissolved within the fluid.
3) $p_{vapL} < p \leq p_{vapU}$: Vapor and fluid are present and the air is completely free.
4) $p \leq p_{vapL}$: Only vapor and air are present.

In all four cases, a measure for the air which is dissolved in the fluid is required. It has been shown that the ratio ζ of the volume of the dissolved air to the overall volume of air and fluid is a good choice [12]. The theoretical volume, which would be incorporated by the air when fully free under normal conditions ($p_0 = 1$ bar) is denoted V_{a0}. The remaining volume of the fluid (again under normal conditions) is not influenced

Post-print version of the article: W. Kemmetmüller, K. Holzmann, A. Kugi, and M. Stork, “Electrorheological Semiactive Shock Isolation Platform for Naval Applications”, *IEEE/ASME Transactions on Mechatronics*, vol. 18, no. 5, pp. 1437–1447, 2013. doi: 10.1109/TMECH.2012.2203456

by this virtual separation and is denoted V_{f0}, thus we have

$$\zeta = \frac{V_{a0}}{V_{a0} + V_{f0}}. \tag{2}$$

Under these assumptions, the theoretical volume of the (separated) fluid and air is called reference volume $V_{r0} = V_{a0} + V_{f0}$. Thus we get

$$V_{a0} = \zeta V_{r0} \tag{3a}$$
$$V_{f0} = (1-\zeta) V_{r0} \, . \tag{3b}$$

The overall mass m consisting of air and fluid is constant and

$$m = V_{a0}\rho_{a0} + V_{f0}\rho_{f0} = \zeta V_{r0}\rho_{a0} + (1-\zeta) V_{r0}\rho_{f0}, \tag{4}$$

holds with the mass densities of air and fluid, ρ_{a0} and ρ_{f0}, both under normal conditions. Furthermore, it is assumed that the air changes its volume isentropically. In the following, the four cases for the description of the fluid are discussed.

1) Case $p_{sat} < p$: In this case the air is completely dissolved within the fluid and does not contribute to the volume. For a constant bulk modulus β_0 (1) yields

$$\rho = \rho_0 e^{\left(\frac{p-p_0}{\beta_0}\right)} \tag{5}$$

and hence the volume V is calculated from the conservation of mass $V_{f0}\rho_{f0} = V\rho$ in the form

$$V = V_{f0} e^{\left(-\frac{p-p_0}{\beta_0}\right)} = (1-\zeta) V_{r0} e^{\left(-\frac{p-p_0}{\beta_0}\right)}, \tag{6}$$

where V_{f0} is the volume of the fluid at normal condition. Making use of (4), one can calculate the mass density

$$\rho = \frac{m}{V} = \left(\frac{\zeta}{(1-\zeta)}\rho_{a0} + \rho_{f0}\right) e^{\left(\frac{p-p_0}{\beta_0}\right)} \, . \tag{7}$$

2) Case $p_{vapU} < p \leq p_{sat}$: In this pressure range a certain part of the air is free. An adapted version of Henry's law is used to determine the percentage of free air [11], [12]. Henry's law basically states that the percentage of dissolved air decreases linearly beginning with 0% at the saturation pressure p_{sat} and reaching 100% at $0\,\mathrm{bar}$. In this article it is, however, assumed that already at the upper saturation vapor pressure p_{vapU} all of the air is free (see, e.g., [11] and [12]). The factor

$$\Theta = \begin{cases} 0 & \text{if} \quad p > p_{sat} \\ 1-\hat{\Theta} & \text{if} \quad p_{vapU} < p \leq p_{sat} \\ 1 & \text{if} \quad p \leq p_{vapU} \end{cases} \tag{8}$$

with

$$\hat{\Theta} = \frac{p - p_{vapU}}{p_{sat} - p_{vapU}} \tag{9}$$

denotes the portion of air which is free at a certain pressure p. As in the first case, a reference volume V_{r0} is considered, which again contains under normal conditions the mass m (4).

If all of the air was free, the pressure p and volume V_a would be related by Poisson's equation for isentropic transitions

$$pV_a^{\kappa_a} = p_0 V_{a0}^{\kappa_a} = \text{const.}, \tag{10}$$

where κ_a is the constant isentropic coefficient of air. Thus, the volume

$$V_a = V_{a0}\left(\frac{p_0}{p}\right)^{\frac{1}{\kappa_a}} \tag{11}$$

is a function of the pressure p. In the considered pressure range only a fraction Θ of the air is free and a portion of $(1-\Theta)$ is dissolved, both under normal conditions. The volume of free air

$$V_a = \Theta V_{a0}\left(\frac{p_0}{p}\right)^{\frac{1}{\kappa_a}} = \Theta\zeta V_{r0}\left(\frac{p_0}{p}\right)^{\frac{1}{\kappa_a}} \, , \tag{12}$$

is calculated based on (3a) and (11) whereas the volume of the remaining dissolved air and the fluid results from (3b) and (6) in the form

$$V_f = V_{f0} e^{\left(-\frac{p-p_0}{\beta_0}\right)} = (1-\zeta) V_{r0} e^{\left(-\frac{p-p_0}{\beta_0}\right)} \, . \tag{13}$$

For the effective density ρ, the relation

$$\rho = \frac{m}{V_a + V_f} = \frac{\zeta\rho_{a0} + (1-\zeta)\rho_{f0}}{\zeta\Theta\left(\frac{p_0}{p}\right)^{\frac{1}{\kappa_a}} + (1-\zeta) e^{\left(-\frac{p-p_0}{\beta_0}\right)}} \tag{14}$$

holds. Using the two abbreviations

$$\beta_a = \zeta\left(\frac{p_0}{p}\right)^{\frac{1}{\kappa_a}} \tag{15a}$$
$$\beta_f = (1-\zeta) e^{\left(-\frac{p-p_0}{\beta_0}\right)} \tag{15b}$$

the effective bulk modulus of the fluid results from (1) and (14) in the form, cf. [12], [10]

$$\beta = \frac{\beta_a\Theta + \beta_f}{\beta_a\left(\frac{\Theta}{\kappa_a p} + \frac{1}{p_{sat} - p_{vapU}}\right) + \frac{\beta_f}{\beta_0}} \, . \tag{16}$$

3) Case $p_{vapL} < p \leq p_{vapU}$: In this case, all the air is free air, i.e. we have $\Theta = 1$. From the upper saturation pressure p_{vapU} the liquid begins to evaporate until the lower saturation pressure p_{vapL} is reached and all the liquid has evaporated. Similar to the percentage Θ of free air in the previous case, the fraction Φ of vaporized liquid can be described in a steady approach with the adapted Henry's law in the range between p_{vapU} and p_{vapL}. Similar to Case 2, the following relation for Φ as a function of the pressure p is used

$$\Phi = \begin{cases} 0 & \text{if} \quad p > p_{vapU} \\ 1-\hat{\Phi} & \text{if} \quad p_{vapL} < p \leq p_{vapU} \\ 1 & \text{if} \quad p \leq p_{vapL} \end{cases} \tag{17}$$

with the abbreviation

$$\hat{\Phi} = \frac{p - p_{vapL}}{p_{vapU} - p_{vapL}} \, . \tag{18}$$

The volume of free air results from (12) with $\Theta = 1$ to

$$V_a = \zeta V_{r0}\left(\frac{p_0}{p}\right)^{\frac{1}{\kappa_a}} \, . \tag{19}$$

The fluid vapor would (under normal conditions as a liquid) incorporate the volume $\Phi(1-\zeta) V_{r0}$, which corresponds to a mass of

$$m_v = \rho_{f0}\Phi(1-\zeta) V_{r0} \, . \tag{20}$$

Post-print version of the article: W. Kemmetmüller, K. Holzmann, A. Kugi, and M. Stork, "Electrorheological Semiactive Shock Isolation Platform for Naval Applications", *IEEE/ASME Transactions on Mechatronics*, vol. 18, no. 5, pp. 1437–1447, 2013. DOI: 10.1109/TMECH.2012.2203456
The content of this post-print version is identical to the published paper but without the publisher's final layout or copy editing.

In the considered pressure range this mass is in the form of vapor and would possess a volume of

$$V_{vvapU} = \frac{m_v}{\rho_{vvapU}} = \frac{\rho_{f0}}{\rho_{vvapU}} \Phi\,(1-\zeta)\,V_{r0} \tag{21}$$

at the upper saturation pressure p_{vapU} with the corresponding density ρ_{vvapU} of the vapor. Again, the isentropic relation (11) holds for the vapor volume

$$V_v = \frac{\rho_{f0}}{\rho_{vvapU}} \Phi\,(1-\zeta)\,V_{r0} \left(\frac{p_{vapU}}{p}\right)^{\frac{1}{\kappa_v}} \tag{22}$$

with the constant isentropic coefficient κ_v of vapor. Together with the corresponding liquid volume

$$V_f = (1-\zeta)\,(1-\Phi)\,V_{r0} e^{\left(-\frac{p-p_0}{\beta_0}\right)} , \tag{23}$$

the effective density results in

$$\rho = \frac{m}{V_a + V_v + V_f} . \tag{24}$$

The effective bulk modulus can now be calculated using (1) and the abbreviations (15) as well as

$$\beta_v = \frac{\rho_{f0}}{\rho_{vvapU}} (1-\zeta) \left(\frac{p_{vapU}}{p}\right)^{\frac{1}{\kappa_v}} \tag{25}$$

in the form

$$\beta = \frac{\beta_a + \Phi\beta_v + (1-\Phi)\,\beta_f}{\frac{\beta_a}{\kappa_a p} + \beta_f \left(\frac{1-\Phi}{\beta_0} + \frac{\partial\Phi}{\partial p}\right) + \beta_v \left(\frac{\Phi}{\kappa_v p} - \frac{\partial\Phi}{\partial p}\right)} . \tag{26}$$

4) Case $p \leq p_{vapL}$: In this last case only vapor and free air is present. The volume of free air V_a and the volume of vapor V_v result from Case 3 for $\Phi = 1$. It follows that the effective density within the considered pressure range takes the form

$$\rho = \frac{\zeta\rho_{a0} + (1-\zeta)\,\rho_{f0}}{\zeta \left(\frac{p_0}{p}\right)^{\frac{1}{\kappa_a}} + \frac{\rho_{f0}}{\rho_{vvapU}} (1-\zeta) \left(\frac{p_{vapU}}{p}\right)^{\frac{1}{\kappa_v}}} \tag{27}$$

and the effective bulk modulus is given by

$$\beta = p\frac{\beta_a + \beta_v}{\left(\frac{\beta_a}{\kappa_a} + \frac{\beta_v}{\kappa_v}\right)} . \tag{28}$$

B. Electrorheological Fluid and Electrorheological Valve

As already mentioned before, the ERF in the absence of an electric field, i.e. in all components but the ER-valve, can be very well described by means of the mathematical model of isentropic fluids as derived in Section III-A. In the ER-valve, the influence of the electric field is, of course, essential, such that an extended constitutive equation for the ERF is required. There are numerous approaches for the modeling of ERFs proposed in literature, which can be basically divided into microscopic and macroscopic models. The microscopic modeling approaches describe the motion and aggregation of particles under the influence of an external electric field, see, e.g., [4] for an overview. Unfortunately, this approach can only be used to model the behavior of a very limited number of particles. In order to design and simulate the behavior of technical devices and applications, macroscopic ER models have to be used instead. Besides purely phenomenological models describing the input-output behavior of ER devices, a systematic macroscopic description of ERFs is possible in the framework of continuum mechanics. In these latter models the ERF is treated as a homogenous continuum, making use of a so-called generalized Cauchy stress tensor, which incorporates the influence of the electric field, see, e.g., [13], [14]. The main advantage of the continuum mechanics approach is that the resulting models are scalable such that, based on simulations, rather precise predictions of the behavior of the real system can be made. This is the reason why this continuum mechanics approach is chosen to model the behavior of the ERF in this paper.

The subsequent mathematical modeling of the ERF and the ER-valve is based on the following assumptions (see, e.g. [13]): (i) the suspension of polarizable particles in the carrier fluid can be treated as a homogenous continuum, (ii) changes in the electric field strength take effect instantaneously and (iii) there are no memory or long-distance effects. Furthermore, the temperature and the mass density are assumed to be constant.

A typical ER-valve is composed of an outer electrode (cylinder of radius R_o) connected to earth and an inner electrode (cylinder of radius R_i) connected to the voltage U, forming an annular gap (see Fig. 3). Since the height $H = R_o - R_i$ of the gap is small compared to the mean radius $R_m = (R_o + R_i)/2$, the ER-valve can be approximated by an equivalent flat channel of the length L and the width $W = 2R_m\pi$.

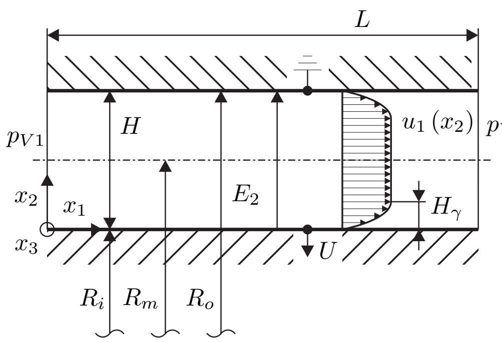

Fig. 3. Longitudinal section of an ER-valve.

Due to the geometry of the valve only laminar flow within the gap has to be considered. Thus, the ERF flows only in x_1-direction, i. e. the velocity $\mathbf{u}$ is given by $\mathbf{u} = u_1(x_2)\,\mathbf{e}_1$, where $\mathbf{e}_1$ is the unit vector in x_1-direction. Furthermore, the electric field $\mathbf{E} = E_2\mathbf{e}_2$ is assumed to act only in x_2-direction and thus perpendicular to the direction of the fluid flow. With the dynamic viscosity η and the field dependent yield strength $\tau_0(E_2)$, the constitutive equation of an extended Bingham model, see, e. g., [13]

$$\sigma_{12} = \tau_0(E_2)\,\mathrm{sign}(\dot\gamma) + \eta\dot\gamma \qquad \text{if} \qquad \dot\gamma \neq 0 \tag{29}$$

can be derived from a more general constituve equation in order to describe the behavior of the ERF inside the gap of the ER-valve, [13], [15]. Here, $\dot\gamma = \partial u_1/\partial x_2$ is the shear rate and σ_{12} is the corresponding shear stress. In the case of

Post-print version of the article: W. Kemmetmüller, K. Holzmann, A. Kugi, and M. Stork, "Electrorheological Semiactive Shock Isolation Platform for Naval Applications", *IEEE/ASME Transactions on Mechatronics*, vol. 18, no. 5, pp. 1437–1447, 2013. DOI: 10.1109/TMECH.2012.2203456
The content of this post-print version is identical to the published paper but without the publisher's final layout or copy editing.

$|\sigma_{12}| < \tau_0(E_2)$, it is assumed that the ERF behaves like a solid.

Calculations on a microscopic scale assuming an ideal dipole-dipole interaction between the polarizable particles predict that the yield strength τ_0 has a quadratic growth with the electric field strength $E_2 = U/H$, see, e. g., [4]. Measurements, however, show that above a certain electric field strength $\bar{E}$ a kind of saturation occurs, which results in a henceforth linear increase of the yield strength with respect to the electric field strength. The ERF used in this project is RheOil [16] from Fludicon GmbH. The approximation of measurement data in the form

$$\tau_0(E_2) = \begin{cases} a_1 E_2 + a_2 E_2^2 + a_3 E_2^3 & \text{if} \quad E_2 < \bar{E} \\ b_0 + b_1 E_2 & \text{if} \quad E_2 \geq \bar{E} \end{cases} \tag{30}$$

yields a very good agreement between measurement and approximation, see Fig. 4.

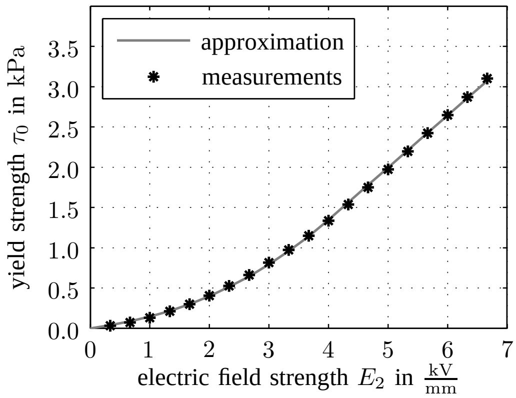

Fig. 4. Comparison of the approximated yield strength τ_0 according to (30) with the measurement values of a test rig.

Using the above constitutive equation of the ERF, the velocity profile can be calculated based on the balance of momentum. For non-vanishing electric fields the resulting velocity profile inside the ER-valve comprises a field dependent plug zone in the middle of the gap, i.e. $\dot{\gamma} = 0$ for $H_\gamma \leq x_2 \leq H - H_\gamma$, where $H_\gamma = H/2 - \tau_0(E_2)/|P|$ and $P = (p_{V1} - p_{V2})/L$ denotes the pressure gradient. In the rest of the gap, the velocity profile is parabolic. The stationary volume flow q_{ER} through the ER-valve is calculated by integration of the velocity profile $u_1(x_2)$ over the area of the gap

$$q_{ER} = \frac{W(|P|H + \tau_0)(|P|H - 2\tau_0)^2}{12P^2\eta}\operatorname{sign}(P) \tag{31}$$

if $|P| > 2\tau_0(E_2)/H$. Otherwise the plug zone covers the whole gap ($H_\gamma = 0$) and the ER-valve is closed, i.e. $q_{ER} = 0$, see, e.g. [15], [17].

The above equation (31) describes the stationary volume flow q_{ER} through the ER-valve. The dynamic behavior of the ER-valve can be approximated based on this stationary relationship by taking into account the effects due to the inertia of the fluid [15]. This results in the following equation for the mass flow $\dot{m}_{ER}$ through the ER-valve

$$\frac{\mathrm{d}}{\mathrm{d}t}\dot{m}_{ER} = \frac{\eta\pi^2}{\rho_{ER}H^2}\left(-\dot{m}_{ER} + \rho_{ER}q_{ER}\right) \tag{32}$$

with the average mass density $\rho_{ER} = \left(\rho(p_{V1}) + \rho(p_{V2})\right)/2$ of the ERF in the gap.

The housing on both sides of the ER-valve are modeled in the form of constant volumes V_{V1} and V_{V2} with the pressures p_{V1} and p_{V2}, respectively. The mass balance for these two volumes results in

$$\frac{\mathrm{d}}{\mathrm{d}t}p_{V1} = \frac{\beta(p_{V1})}{V_{V1}\rho(p_{V1})}\left(\dot{m}_1 - \dot{m}_{ER}\right), \tag{33a}$$

$$\frac{\mathrm{d}}{\mathrm{d}t}p_{V2} = \frac{\beta(p_{V2})}{V_{V2}\rho(p_{V2})}\left(\dot{m}_{ER} - \dot{m}_2\right). \tag{33b}$$

The mass densities $\rho(p_{V1})$ and $\rho(p_{V2})$ and the bulk moduli $\beta(p_{V1})$ and $\beta(p_{V2})$ are determined according to Section III-A since no voltage is applied to the ERF outside the ER-valve.

C. Bypass Throttle and Piping

The determination of the mass flows $\dot{m}_1$ and $\dot{m}_2$ requires a closer examination of the piping of the system. Due to the high accelerations of the base plate and the resulting large changes in the volume flows in the system, the piping has an essential influence on the system dynamics and therefore cannot be neglected. To keep the resulting mathematical model simple, and since wave propagation effects do not play a role in the present application, an approximation in the form of lumped parameter elements is used. The inertia and the resistance are the dominating effects inside the pipes, whereas the compressibility of the fluid can be neglected. In the following, the index $j = 1, 2$ refers to the pipe element associated with the mass flow $\dot{m}_j$ according to Fig. 2. The pressure drop along a pipe element is composed of the inertia term [7], [18]

$$\Delta p_{Ij} = \frac{L_{Pj}}{A_{Pj}}\frac{\mathrm{d}}{\mathrm{d}t}\dot{m}_j \tag{34}$$

and the (turbulent) friction term [18]

$$\Delta p_{Fj} = \frac{\lambda_{Pj}L_{Pj}}{D_{Pj}}\frac{\dot{m}_j^2}{2\rho_{Pj}A_{Pj}^2}\operatorname{sign}(\dot{m}_j) \tag{35}$$

with the friction factor λ_{Pj}, the mass density $\rho_{Pj} = \left(\rho(p_{Vj}) + \rho(p_j)\right)/2$ of the ERF, the length L_{Pj}, the inner diameter D_{Pj} and the cross sectional area A_{Pj} of the pipe. Additional pressure drops due to inlet, outlet and elbows are summarized as

$$\Delta p_{Ej} = \frac{\xi_{Ej}}{2}\frac{\dot{m}_j^2}{\rho_{Pj}A_{Pj}^2}\operatorname{sign}(\dot{m}_j) \tag{36}$$

with the effective pressure loss coefficient ξ_{Ej}, see, e.g., [18]. Thus, the differential equation of the mass flows $\dot{m}_1$ and $\dot{m}_2$ yield

$$\frac{\mathrm{d}}{\mathrm{d}t}\dot{m}_1 = \frac{A_{P1}}{L_{P1}}\left(p_1 - p_{V1} - (\Delta p_{E1} + \Delta p_{F1})\right), \tag{37a}$$

$$\frac{\mathrm{d}}{\mathrm{d}t}\dot{m}_2 = \frac{A_{P2}}{L_{P2}}\left(p_{V2} - p_2 - (\Delta p_{E2} + \Delta p_{F2})\right). \tag{37b}$$

Post-print version of the article: W. Kemmetmüller, K. Holzmann, A. Kugi, and M. Stork, "Electrorheological Semiactive Shock Isolation Platform for Naval Applications", *IEEE/ASME Transactions on Mechatronics*, vol. 18, no. 5, pp. 1437–1447, 2013. DOI: 10.1109/TMECH.2012.2203456
The content of this post-print version is identical to the published paper but without the publisher's final layout or copy editing.

As described in Section II, the bypass throttle ensures the required damping of the platform in normal operation. Furthermore, it is responsible for the fast repositioning of the platform when using the control strategy proposed in Section IV. A throttle with laminar characteristics would be preferable from a theoretical point of view since the resulting damping of the semi-active damper would be proportional to the velocity. Laminar throttles have, however, two major drawbacks: (i) A compact design is not possible and the characteristics is strongly dependent on the viscosity of the fluid. Since the viscosity changes significantly with the temperature of the fluid, this in turn also changes the damping of the system. (ii) It is almost impossible to change the geometry of laminar throttle during measurement campaigns. Thus, a simple adjustment of the damping is not possible. For these reasons, a turbulent throttle, which allows a fast manual adaptation of its flow characteristics during measurement campaigns, was chosen for the prototype. The stationary pressure drop across the bypass throttle [9]

$$\Delta p_T = \frac{\dot{m}_T^2}{2\rho_T \alpha_T^2 A_T^2} \mathrm{sign}\left(\dot{m}_T\right) \tag{38}$$

is a function of the discharge coefficient α_T, the (variable) area A_T of the orifice and the mass flow $\dot{m}_T$ through it. The piping of the turbulent bypass throttle is modeled in the same way as before, dividing the pressure drop across the pipe in the friction term Δp_{FT} and the pressure drops due to inlet, outlet and elbows Δp_{ET}.

$$\frac{\mathrm{d}}{\mathrm{d}t}\dot{m}_T = \frac{A_{PT}}{L_{PT}}\left(p_1 - p_2 - \left(\Delta p_{FT} + \Delta p_{ET} + \Delta p_T\right)\right) \tag{39}$$

Here, the mass density $\rho_T = \left(\rho\left(p_1\right) + \rho\left(p_2\right)\right)/2$, the length L_{PT} and the cross sectional area A_{PT} of the pipe are used.

D. Platform

As only the absolute value of the acceleration a_P of the platform but not the absolute values of its velocity or position are of interest, it is reasonable to use the relative position $\Delta z = z_P - z_B$ and relative velocity $\Delta v = v_P - v_B$ as new state variables. The conservation of momentum yields the mathematical model of the platform

$$\frac{\mathrm{d}}{\mathrm{d}t}\Delta z = \Delta v \tag{40a}$$

$$\frac{\mathrm{d}}{\mathrm{d}t}\Delta v = a_P - a_B \tag{40b}$$

where the acceleration

$$a_P = \frac{4}{m_P + m_L}\left(F_A\left(\Delta z\right) + F_D\left(p_1 - p_2\right)\right) - g \tag{41}$$

is a function of the damper force F_D depending on the pressure difference $p_1 - p_2$ and the air spring force F_A depending on the relative position Δz. Furthermore, $g = 9.81 \frac{\mathrm{m}}{\mathrm{s}^2}$ denotes the gravitational constant and m_P and m_L denote the mass of the platform and its payload, respectively.

E. Damping Cylinder

The high accelerations during the shock lead to a pressure gradient within the chambers of the damping cylinder which could be modeled by means of partial differential equations. It turns out that for the purpose of analysis and design of the shock isolation platform a lumped parameter model with homogenous chamber pressures p_1 and p_2 is sufficient. The internal leakage between chamber 1 and 2 can be described by the mass flow

$$\dot{m}_{l,12} = k_{l,12}\left(p_1 - p_2\right)\frac{\rho\left(p_1\right) + \rho\left(p_2\right)}{2} \tag{42}$$

with the laminar leakage coefficient $k_{l,12}$ and the mass densities $\rho\left(p_1\right)$ and $\rho\left(p_2\right)$ of the ERF in the two cylinder chambers. The external leakages can be neglected due to the good sealing. With the initial volumes V_{10} and V_{20} of the damping cylinder and the effective piston area A_K, the differential equations for the chamber pressures take the form

$$\frac{\mathrm{d}}{\mathrm{d}t}p_1 = \frac{\beta\left(p_1\right)}{V_{10} + \Delta z A_K}\left(-\frac{\dot{m}_1 + \dot{m}_{l,12} + \dot{m}_T}{\rho\left(p_1\right)} - \Delta v A_K\right) \tag{43a}$$

$$\frac{\mathrm{d}}{\mathrm{d}t}p_2 = \frac{\beta\left(p_2\right)}{V_{20} - \Delta z A_K}\left(\frac{\dot{m}_2 + \dot{m}_{l,12} + \dot{m}_T}{\rho\left(p_2\right)} + \Delta v A_K\right) . \tag{43b}$$

The mass densities $\rho\left(p_1\right)$ and $\rho\left(p_2\right)$ and the bulk moduli $\beta\left(p_1\right)$ and $\beta\left(p_2\right)$ are calculated according Section III-A since the high accelerations during the shock event can cause cavitation within the system. The overall damper force is given by

$$F_D = A_K\left(p_1 - p_2\right) + F_R, \tag{44}$$

where F_R summarizes the mechanical friction of the damping cylinder.

F. Air Spring

For the subsequent simulation studies it is assumed that the movement of the air spring is sufficiently fast. This assumption entails that the heat exchange with the environment can be neglected and therefore the thermodynamic process can be regarded as isentropic. With the pre-charge pressure p_{A0} and the corresponding air volume V_{A0}, the pressure in the air spring can be calculated as follows

$$p_A\left(\Delta z\right) = p_{A0}\left(\frac{V_{A0}}{V_A\left(\Delta z\right)}\right)^{\kappa_a} \tag{45}$$

with the air volume $V_A\left(\Delta z\right)$ and the isentropic coefficient κ_a of air. The resulting force of the air spring [19]

$$F_A\left(\Delta z\right) = p_A\left(\Delta z\right)\frac{D_A^2\left(\Delta z\right)\pi}{4} \tag{46}$$

is determined by the effective diameter $D_A\left(\Delta z\right)$.

Post-print version of the article: W. Kemmetmüller, K. Holzmann, A. Kugi, and M. Stork, “Electrorheological Semiactive Shock Isolation Platform for Naval Applications”, *IEEE/ASME Transactions on Mechatronics*, vol. 18, no. 5, pp. 1437–1447, 2013. DOI: 10.1109/TMECH.2012.2203456
The content of this post-print version is identical to the published paper but without the publisher’s final layout or copy editing.

IV. Control Strategy

The characteristics of the spring is defined by the choice of the air spring. Thus, the only possible control input is the damping characteristics determined by the applied voltage U. Nevertheless, in the sense of a mechatronic design approach, the choice of the spring has been regarded as an extra degree-of-freedom in the design of the system. Here, basically the following consideration have been used for the choice of the spring: (i) The spring has to support the static weight of the load and the platform. (ii) In order to ensure small acceleration of the platform, the stiffness of the spring should be kept as low as possible. (iii) On the other hand, high stiffness is necessary in order to guarantee a fast repositioning of the platform after the shock. Based on simulation results, the parameters of the spring have been chosen such that a good compromise between the conflicting demands (ii) and (iii) has been reached.

The demands on the control strategy can be summarized as follows: (i) Under normal operation conditions, the damping should be high in order to avoid undesired oscillations of the platform. (ii) In case of a shock, the damping has to be sufficiently small to assure minimum acceleration a_P of the platform. (iii) After the shock, the induced oscillation of the platform should be damped rapidly and the relative distance between the base plate and the platform should be within a certain limit.

This directly leads to the following control strategy:

1) Under normal conditions, the ER-valve is completely closed by applying the maximum voltage of $U = 6\,\mathrm{kV}$. The damping of the system is then defined by the bypass throttle.
2) Upon detection of a shock, i.e. when the excitation a_B exceeds a certain threshold, the voltage on the ER-valve is removed resulting in minimum pressure difference and thus minimum force of the damping cylinder.
3) When a certain time period ΔT_S, which is characteristic for shocks caused by weaponry impact, has passed after detection of the shock, the maximum voltage of $U = 6\,\mathrm{kV}$ is applied again. This results in high damping forces which are responsible for the fast repositioning of the platform.

One main advantage of this control strategy is its simplicity. Only one acceleration sensor mounted on the base plate is necessary to implement the control strategy. Secondly, this control strategy is also optimal in case of a shock since the accelerations on the platform are minimized.

Furthermore, the basic functionality of the shock isolation platform is also preserved in case of a failure of the power supply. In this case, the shock isolation characteristics is not changed at all. During normal operation, however, the damping of the platform is lower than normal which yields to large oscillations. Nevertheless, the remaining damping of the system is sufficient for a basic operation of the platform.

The possible failure of the shock isolation platform is a shock event, which remains undetected due to a failure of the sensor. In this case, the voltage $U = 6\,\mathrm{kV}$ is applied to the ER damper all the time. This leads to higher accelerations a_P on the platform which are, however, still much smaller than the acceleration on the base plate. Thus, also in this second scenario the basic shock isolation functionality is preserved.

TABLE I
Parameters of the four parallel ER-valves at each corner.

Parameter	Value	Unit
H	1	mm
L	200	mm
R_m	35	mm

V. Simulation Study

The mathematical model used for the simulations has been derived and described in Section III of this work. Four ER-valves, each with the dimensions as presented in Table I, are connected in parallel at each corner of the platform in order to provide a sufficiently large area for the enormous volume flows during a shock event. The mass of the platform is estimated with $m_P = 900\,\mathrm{kg}$ and a payload of $m_L = 400\,\mathrm{kg}$ was given as nominal value. A block diagram of the overall simulation model is presented in Fig. 5. Furthermore, the typical time span of the shock a_B is given by $\Delta T_S = 20\,\mathrm{ms}$, see Fig. 6.

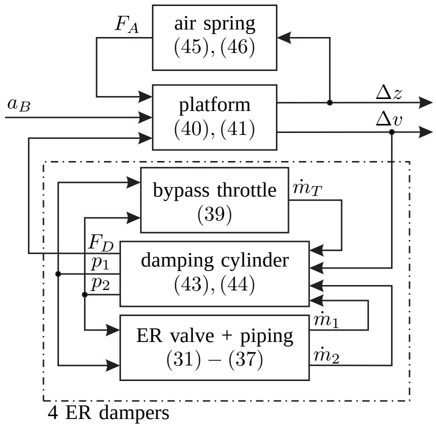

Fig. 5. Block diagram of the simulation model derived in Section III.

The simulations are based on a benchmark excitation a_B on the base plate which is typical for the excitations in naval applications due to weaponry impact, cf. Fig. 6. In this figure, the resulting acceleration a_P of the platform during the shock is depicted together with the excitation a_B of the base plate (ship). The peak value of the excitation of $3000\,\frac{\mathrm{m}}{\mathrm{s}^2}$ is reduced to a value of approximately $60\,\frac{\mathrm{m}}{\mathrm{s}^2}$ at the platform, which is a reduction of nearly a factor 50.

The corresponding relative displacement Δz is presented in Fig. 7. The platform reaches its rest point after $0.27\,\mathrm{s}$, which is a very good result when imaging the size of the prototype. Due to static friction in the system an exact repositioning is not possible and the repositioning error is approximately $1.7\,\mathrm{mm}$.

The forces,acting on each of the four corners of the platform, are depicted in Fig. 8. One can see the high damping force F_D occurring at the very beginning, i.e. during the shock

Post-print version of the article: W. Kemmetmüller, K. Holzmann, A. Kugi, and M. Stork, "Electrorheological Semiactive Shock Isolation Platform for Naval Applications", *IEEE/ASME Transactions on Mechatronics*, vol. 18, no. 5, pp. 1437–1447, 2013. doi: 10.1109/TMECH.2012.2203456
The content of this post-print version is identical to the published paper but without the publisher's final layout or copy editing.

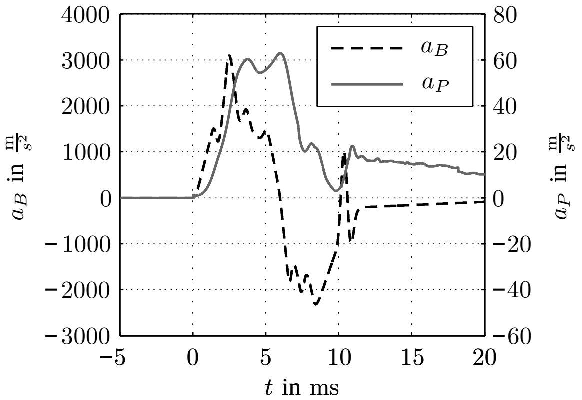

Fig. 6. Acceleration a_B on the base plate and a_P on the platform.

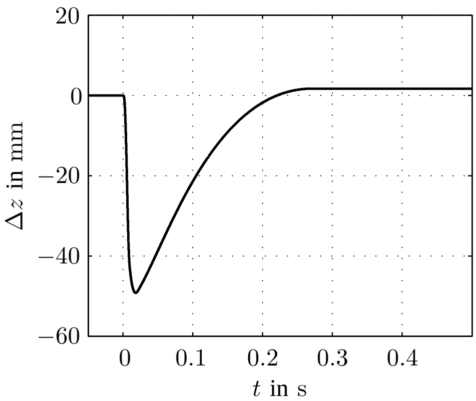

Fig. 7. Relative displacement Δz.

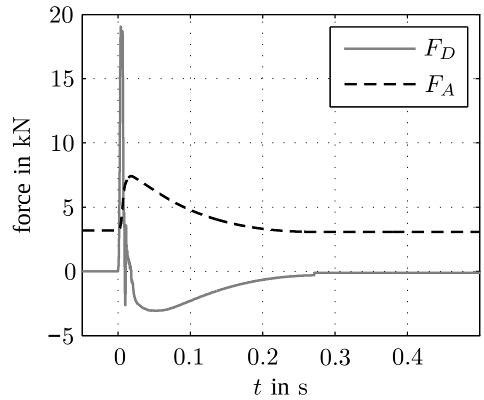

Fig. 8. Force F_D of the damping cylinder and F_A of the air spring.

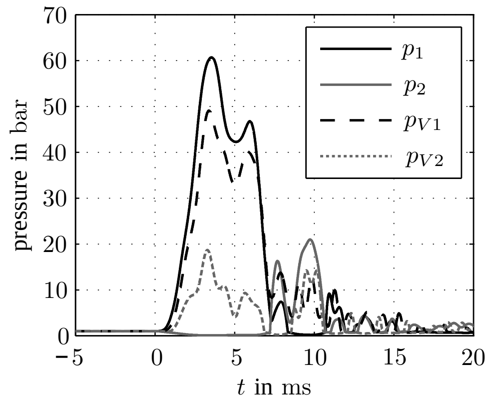

Fig. 9. Pressures p_1, p_2, p_{V1} and p_{V2} according to Fig. 2.

due to the high accelerations and velocities while the force F_A of the air spring is only a function of the relative displacement Δz and thus significant smaller. The damping force starts with $F_D = 0\,\text{N}$ before the shock since no relative motion exists while at the same time the air spring has to compensate the mass $m_P = 900\,\text{kg}$ of the platform and its payload of $m_L = 400\,\text{kg}$. One can identify a sudden change in the damping force when the platform comes to rest at $t \approx 0.27\,\text{s}$ which is due to the friction in the damping cylinder.

The damping force is mainly determined by the pressures p_1 and p_2 in the chambers. They are, together with the pressures p_{V1} and p_{V2}, illustrated in Fig. 9. The maximum pressure occurring in chamber 1 is approximately 61 bar. Whereas the pressures in the chambers and the adjacent constant volumes are different immediately after the shock, they are nearly identical after the fast transients have decayed. Looking at p_2, one can clearly identify the drop below $p_0 = 1\,\text{bar}$ which conforms with the isentropic fluid model of Section III-A.

VI. Measurement Results

In order to prove the function of the prototype depicted in Fig. 10, measurements were performed on a shock test-bench at the Bundeswehr Technical Center for Ships and Naval Weapons (WTD 71) in Kiel, Germany.

This test-bench is designed for the shock test of military systems and can produce vertical acceleration a_B in the order of $240\,g$. The excitations produced by the test-bench are slightly different compared to the measured excitations of a real weaponry impact used in the simulation studies in Section V. Thus, a direct comparison of the simulation and measurement results is not possible. The basic features of the shock isolation platform can, however, also be tested by means of the test-bench. Two different scenarios with a payload of $m_L = 800\,\text{kg}$ were examined during the tests, one nominal scenario with control of the ER dampers and one scenario without control, i.e. with no voltage applied to the ER dampers.

The evaluation of the measurement results is based on a comparison of the acceleration a_B applied to the base plate with the resultant acceleration a_P on the platform. The smaller a_P, the better is the shock isolation, see Fig. 11. An excitation of $a_B \approx 2400\,\frac{\text{m}}{\text{s}^2}$ leads to an acceleration a_P of approximately $125\,\frac{\text{m}}{\text{s}^2}$.

A comparison of the post-shock oscillation times in Fig. 11 shows the advantage of the control strategy. In the case without control it takes approximately $1.1\,\text{s}$ for the platform to come to rest. This can be significantly improved when applying the control strategy which reduces the post-shock oscillation time to approximately $0.6\,\text{s}$. It can be easily seen that the control

Post-print version of the article: W. Kemmetmüller, K. Holzmann, A. Kugi, and M. Stork, "Electrorheological Semiactive Shock Isolation Platform for Naval Applications", *IEEE/ASME Transactions on Mechatronics*, vol. 18, no. 5, pp. 1437–1447, 2013. DOI: 10.1109/TMECH.2012.2203456
The content of this post-print version is identical to the published paper but without the publisher's final layout or copy editing.

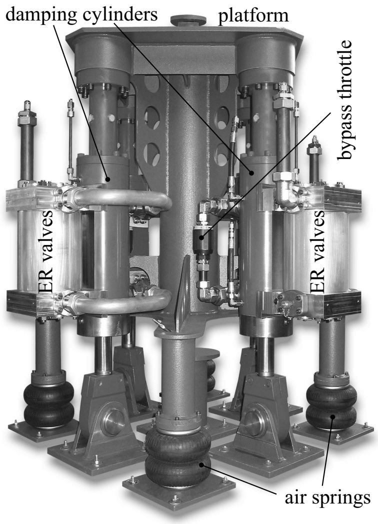

Fig. 10. Photo of the prototype, source: Fludicon GmbH.

leads to a significant reduction of the post-shock oscillation time while not increasing the resultant acceleration on the platform.

VII. Conclusion

This contribution presents a semi-active shock isolation platform for naval applications making use of the special properties of electrorheological fluids. The primary objective is the significant reduction of induced accelerations while assuring a fast and accurate repositioning of the platform. A control strategy was proposed, which uses only one acceleration sensor to fulfill these requirements. Simulation studies based on a benchmark excitation proved the proper functionality of the system. A peak value of the excitation of $3000\,\frac{\mathrm{m}}{\mathrm{s}^2}$ could be reduced almost by the factor 50 which is a satisfying value for the intended employment. Furthermore, measurements on a shock test-bench were performed, validating these good results.

Acknowledgment

The authors would like to thank Steffen Schneider from the Bundeswehr Research Institute for Materials, Fuels and Lubricants (WIWeB), Erding, Germany for many fruitful technical discussions and Sven Diedrichsen from the Bundeswehr Technical Center for Ships and Naval Weapons (WTD 71), Eckernförde, Germany for supporting the measurement campaigns.

References

[1] C. Harris and C. Crede, Eds., *Shock and Vibration Handbook, Vol 1: Basic Theory and Measurements*. New York, USA: McGraw-Hill, 1961.
[2] *Military Equipment Shock and Vibration Solutions*, Enidine Incorporated, New York, USA, 2008.
[3] C. M. Harris and C. E. Crede, Eds., *Shock and Vibration Handbook, Vol 2: Data Analysis, Testing, and Methods of Control*. New York, USA: McGraw-Hill, 1961.
[4] M. Parthasarathy and D. J. Klingenberg, "Electrorheology: Mechanisms and models," *J. Materials Science and Engineering R*, vol. 17, pp. 57–103, 1996.
[5] A. Kugi, K. Holzmann, and W. Kemmetmüller, "Active and Semi-active Control of Electrorheological Fluid Devices," in *IUTAM Symp. on Vibration Control of Nonlinear Mechanisms and Structures*, H. Ulbrich and W. Günthner, Eds. Dordrecht, Netherlands: Springer, 2005, pp. 203–212.
[6] K. Holzmann, W. Kemmetmüller, A. Kugi, M. Stork, H. Rosenfeldt, and S. Schneider, "Modeling and control of an off-road truck using electrorheological dampers," in *J. of Physics: Conference Series*, vol. 149, no. 012011, 2009.
[7] J. F. Blackburn, G. Reethof, and J. L. Shearer, *Fluid Power Control*. New York, USA: John Wiley & Sons, 1960.
[8] N. D. Manring, *Hydraulic Control Systems*. New York, USA: John Wiley & Sons, 2005.
[9] H. E. Merritt, *Hydraulic Control Systems*. New York, USA: John Wiley & Sons, 1967.
[10] J. P. Franc, F. Avellan, B. Belahadji, J. Y. Billard, L. Briançon-Marjollet, D. Fréchou, D. H. Fruman, A. Karimi, J. L. Kueny, and J. M. Michel, *La Cavitation: Mécanismes Physiques et Aspects Industriels*. Grenoble, France: Presses universitaires de Grenoble PUG, 1995.
[11] P. Casoli, A. Vacca, G. Franzoni, and G. L. Berta, "Modelling of fluid properties in hydraulic positive displacement machines," *Simulation Modelling Practice and Theory*, vol. 14, pp. 1059–1072, 2006.
[12] *AMESim Standard fluid properties TB117*, Imagine, Roanne, France, 2000.
[13] K. R. Rajagopal and A. S. Wineman, "Flow of Electro-rheological Material," *Acta Mechanica*, vol. 91, pp. 57–75, 1992.
[14] M. Růžička, *Electrorheological Fluids: Modeling and Mathematical Theory*. Berlin, Germany: Springer, 2000.
[15] W. Kemmetmüller, *Mathematical Modeling and Nonlinear Control of Electrohydraulic and Electrorheological Systems*. Aachen, Germany: Shaker, 2008.
[16] *RheOil 2.6*, Fludicon GmbH, Darmstadt, Germany, April 2005.
[17] W. Kemmetmüller and A. Kugi, "Modeling and Control of an Electrorheological Actuator," in *Proc. 3rd IFAC Symp. on Mechatronic Systems*, Sydney, Australia, 2004, pp. 271–276.
[18] M. Rabie, *Fluid Power Engineering*. New York, USA: McGraw-Hill, 2009.
[19] *Application of ContiTech air springs*, ContiTech Luftfedersysteme GmbH, Hannover, Germany.

Wolfgang Kemmetmüller (M'04) received the Dipl.-Ing. degree in mechatronics from the Johannes Kepler University Linz, Austria, in 2002 and his Ph.D. (Dr.-Ing.) degree in control engineering from Saarland University, Saarbruecken, Germany, in 2007. From 2002 to 2007 he worked as a research assistant at the Chair of System Theory and Automatic Control at Saarland University. Since 2007 he is a senior researcher at the Automation and Control Institute at Vienna University of Technology, Vienna, Austria. His research interests include the physics based modeling and the nonlinear control of mechatronic systems with a special focus on electrorheological and electrohydraulics systems where he is involved in several industrial research projects. Dr. Kemmetmüller is associate editor of the IFAC journal Mechatronics.

Post-print version of the article: W. Kemmetmüller, K. Holzmann, A. Kugi, and M. Stork, "Electrorheological Semiactive Shock Isolation Platform for Naval Applications", *IEEE/ASME Transactions on Mechatronics*, vol. 18, no. 5, pp. 1437–1447, 2013. doi: 10.1109/TMECH.2012.2203456
The content of this post-print version is identical to the published paper but without the publisher's final layout or copy editing.

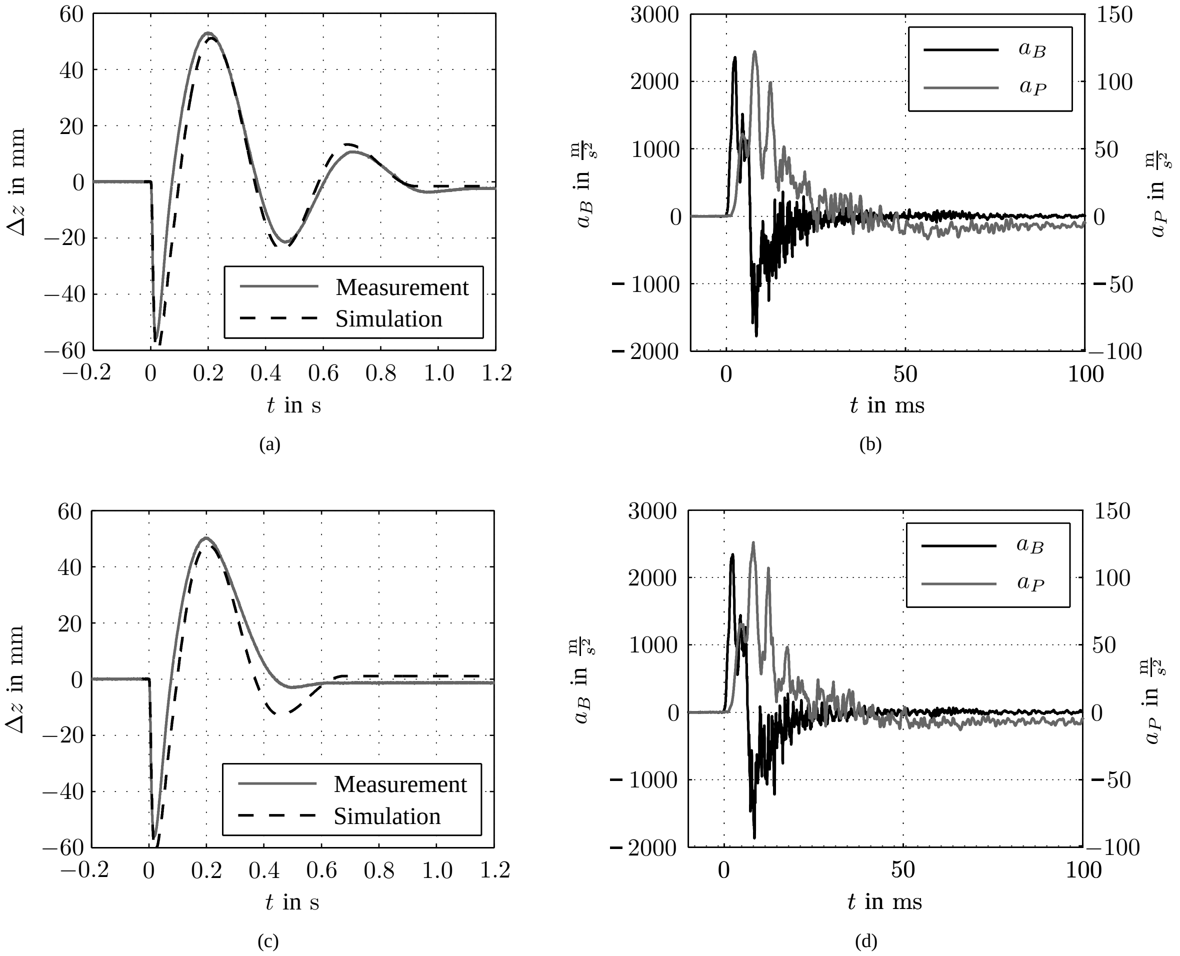

Fig. 11. Relative displacement Δz in (a) without control ($U = 0\,\mathrm{kV}$) and in (c) with control. Measurement values of the acceleration a_B on the base plate and on the platform a_P in (b) without control and in (d) with control.

Klaus Holzmann received the MSc. degree in mechatronics from the Loughborough University, Loughborough, U.K., in 2002, the Dipl.-Ing. degree in mechatronics from the Johannes Kepler University, Linz, Austria, in 2004 and the Ph.D. (Dr. techn.) degree from Vienna University of Technology in 2011, respectively. Between March 2004 and May 2007, he worked as a research assistant at the Chair of System Theory and Automatic Control, Saarland University, Saarbruecken, Germany. From June 2007 to August 2008, he continued his research at the Automation and Control Institute (ACIN), Vienna University of Technology, Vienna, Austria. Since September 2008, he is Head of Control Engineering at Fludicon GmbH, Darmstadt, Germany. His research interests include the mathematical modeling and control of electrorheological dampers and systems.

Andreas Kugi (M'94) received the Dipl.-Ing. degree in electrical engineering from Graz University of Technology, Austria, and the Ph.D. (Dr. techn.) degree in control engineering from Johannes Kepler University (JKU), Linz, Austria, in 1992 and 1995, respectively. From 1995 to 2000 he worked as an assistant professor and from 2000 to 2002 as an associate professor at JKU. He received his "Habilitation" degree in the field of automatic control and control theory from JKU in 2000. In 2002, he was appointed full professor at Saarland University, Saarbrücken, Germany, where he held the Chair of System Theory and Automatic Control until May 2007. Since June 2007 he is a full professor for complex dynamical systems and head of the Automation and Control Institute at Vienna University of Technology, Austria.

His research interests include the physics-based modeling and control of (nonlinear) mechatronic systems, differential geometric and algebraic methods for nonlinear control, and the controller design for infinite-dimensional systems. He is involved in several industrial research projects in the field of automotive applications, hydraulic servo-drives, smart structures and rolling mill applications. Prof. Kugi is Editor-in Chief of the IFAC journal Control Engineering Practice and since 2010 he is corresponding member of the Austrian Academy of Sciences.

Post-print version of the article: W. Kemmetmüller, K. Holzmann, A. Kugi, and M. Stork, "Electrorheological Semiactive Shock Isolation Platform for Naval Applications", *IEEE/ASME Transactions on Mechatronics*, vol. 18, no. 5, pp. 1437–1447, 2013. DOI: 10.1109/TMECH.2012.2203456
The content of this post-print version is identical to the published paper but without the publisher's final layout or copy editing.

Michael Stork recieved his Dipl-Ing. degree in mechanical engineering from Darmstadt University of Technology, Germany, in 1986. He worked as a development engineer at Carl Schenck AG in Darmstadt, division balancing machines. In 1992 he took over the head management of the mechanical development department at Carl Schenck AG, later on at Schenck RoTec GmbH. In 2002 he worked for Schenck RoTec GmbH in the department technology and innovation. In 2003 he moved to FLUDICON GmbH Darmstadt as CTO, where he is responsible for the business unit industry.

Post-print version of the article: W. Kemmetmüller, K. Holzmann, A. Kugi, and M. Stork, "Electrorheological Semiactive Shock Isolation Platform for Naval Applications", *IEEE/ASME Transactions on Mechatronics*, vol. 18, no. 5, pp. 1437–1447, 2013. DOI: 10.1109/TMECH.2012.2203456
The content of this post-print version is identical to the published paper but without the publisher's final layout or copy editing.